Compressible Cake Characterization from Steady-State Filtration Analysis

Peter Kovalsky, Marion Gedrat, and Graeme Bushell
Particle and Catalysis Research Group, School of Chemical Sciences and Engineering, University of New South Wales, Sydney, NSW 2052, Australia

T. David Waite
Centre for Water and Waste Technology, School of Civil and Environmental Engineering, University of New South Wales, Sydney, NSW 2052, Australia

DOI 10.1002/aic.11193
Published online May 7, 2007 in Wiley InterScience (www.interscience.wiley.com).

A numerical technique for quantifying the key material properties that describe how a flocculated suspension behaves under constant pressure filtration is presented with unrestricted compressive yield stress and permeability models used to describe these material properties. Using an iterative procedure, the optimal parameters for these models are calculated as are pressure and solid fraction distribution profiles. Input parameters to the numerical analysis are flux and final cake height data obtained from batch filtration experiments, which are driven to steady-state. This technique is validated against piston driven filtration (odeometer) and centrifuge experiments for zirconia, soil particles, and yeast assemblages. The compressive yield stress calculated from filtration experiments agrees well with values obtained by odeometer and centrifuge studies for all particle systems studied at both the low and high solid pressure regions. Similarly, the calculated permeability agrees well with the measured permeability. © 2007 American Institute of Chemical Engineers *AIChE J,* 53: 1483–1495, 2007
Keywords: filtration, flocculation, dewatering, compressive yield stress, permeability, local cake properties

Introduction

Despite the huge amount of work that has been undertaken,[1–3] the manner in which flocculated particles behave under compression is yet to be well understood. When compressed beyond the gel point, flocculated materials will tend to consolidate, with the extent of volume reduction dependent among other things, on the interparticle bond strength. In many cases, extensive consolidation leads to transformation from a high porosity, high permeability system to a low porosity, low permeability system while in others (such as swelling clays), high porosity yet low permeability is maintained due to the gel-like nature of the material and its resistance to consolidation. To complicate the issue further, the pressure exerted on the solids is nonuniform and a gradation in extent of consolidation is observed in the direction of increasing solid pressure. Being able to quantify features such as the local permeability and compressibility of a material and to assess the impact of these properties on the macroscopic behavior of the consolidated material is of industrial significance. For example, understanding the connection between flocculant choice and operating conditions and the resulting impact on the material properties of the resulting accumulated solid or "cake" is critical in performance of processes such as sludge dewatering and membrane filtration.

Motivation for the study

In this work, a numerical technique for assessing the filterability of a flocculated system based on laboratory scale

Correspondence concerning this article should be addressed to G. Bushell at g.bushell@unsw.edu.au.

dead-end filtration data is demonstrated using the approach and terminology adopted by soil physicists and membrane filtration specialists interested in water flux through consolidated porous solids.

The approach adopted here is based upon the observation that solid loadings in drinking water filtration are relatively low (<100 ppm). Over short time scales at least, one can assume that the accumulation of new material onto a cake is negligible, with the cake reaching a pseudo-steady state (with respect to thickness and material properties) in response to operating pressure changes. We are particularly interested in the extent of consolidation of the cake at steady-state and the flux through this consolidated cake.

In this work, we also address the complexities of modeling filtration in gas driven filtration systems under conditions typical of those encountered in low pressure submerged membrane filtration. We propose that the technique developed here could be utilized as an in situ tool for measuring the dewatering (consolidation) properties of the suspended material based on real plant filtration data.

Availability of an in situ method for characterizing the material properties of raw water is important to ascertain the characteristics of the material that contributes to poor filterability. It may also be possible to predict the cut-off flux (i.e., the point at which an increase in pressure leads to a decrease in throughput) based on the materials dewatering properties. This is particularly important for constant flux filtration and optimization of the frequency and intensity of filter cleaning.

The approach described here is a numerical technique for quantifying the dewatering properties of a material which, concomitantly, enables determination of the extent of consolidation during filtration. The key dewatering properties are the permeability (ease of fluid passage through the cake) and compressibility (a measure of the strength of the particle network). The technique is based on the assumption of potentially reasonable permeability $K(\phi)$ and compressive yield stress $P_Y(\phi)$ functions. Evaluation of the accuracy of the assumed functions is undertaken by substituting these functions into a momentum balance equation and integrating across the cake to compare the calculated pressure drop with the actual measured pressure drop. A convergence process is required to select parameters for $K(\phi)$ and $P_Y(\phi)$ such that the difference between the measured and predicted pressure drops is minimized.

Traditional cake modeling

The classical filtration equation derived from Darcy's Law[4] relates flux (J) through a porous medium covered in a porous cake to both the pressure applied across the filtration medium (ΔP) and the resistance of the cake (R_c) and membrane (R_m):

$$J = \frac{1}{A_c}\frac{dV}{dt} = \frac{\Delta P}{\mu(R_c + R_m)} \tag{1}$$

where J is defined as the rate of change of cumulative filtrate volume V per area A_c and μ is fluid viscosity. The assumption is made that the resistance of the cake layer is directly proportional to the amount of mass deposited on the filter with mass accumulating in direct proportion to the volume of suspension filtered; i.e.

$$R_c = \alpha\frac{c_s V}{A_c} \tag{2}$$

where α is the specific cake resistance and c_s is the solid volume concentration.

Added complexity arises for materials that are compressible. To account for this it is necessary to address how the permeability of cake changes with pressure. Tiller proposes the following model for the average specific cake resistance[5]

$$\alpha_{av} = \alpha_o \Delta P^N \tag{3}$$

where α_o is the specific resistance at some nominal pressure, ΔP is the difference between the applied pressure and nominal pressure, and N is an indication of the cake compressibility. Typically, the value of N is measured experimentally.

For modeling the filtration behavior of highly compressible material such as those developed from flocs, this approach has real limitations as there is likely to be significant variation from the average specific resistance within the cake, particularly as a gradient in pressure through the cake is to be expected. It is thus necessary to analyze compressible cakes based on local cake properties rather than average cake properties, however such analysis is relatively complex if undertaken whilst the cake mass is increasing and undergoing consolidation. The problem is simplified here by considering a steady-state filtration approach in which cake mass is constant and consolidation has ceased.

Recent work on cake characterization

Investigators concerned with the optimization of the performance of filter presses have given particular attention to the characterization of cakes formed from highly compressible material.[6] Variation in cake properties with time is commonly described by the momentum balance for the filtration process,[7] i.e.

$$\frac{\partial\phi}{\partial t} = \frac{\partial}{\partial z}\left[D(\phi)\frac{\partial\phi}{\partial z} - \phi\frac{\partial H}{\partial t}\right] \tag{4}$$

where ϕ is the solid volume fraction, z is the distance in the direction of cake formation, t is time, H is cake height, and D is cake diffusivity (which is a function of solid volume fraction). By solution of Eq. 4, it is possible to deduce the local cake properties.

Several authors propose solutions to this momentum balance equation. Landman et al.[8] proposes a solution using a similarity substitution to obtain an equation for the cumulative outflow of the form

$$V = \beta t^{\frac{1}{2}} \tag{5}$$

where V is the outflow due to consolidation of the cake and β is obtained from the slope of a t/V versus V curve. It is important to note that this equation will only be valid where the outflow is exclusively due to collapse in the cake and not

due to the additional contribution from supernatant passing through the cake. This may well occur when the initial suspension consolidates/settles under its own weight leaving a layer of clear supernatant above which is subsequently pushed through the cake. In this situation, the experimentally derived value of β could potentially be overestimated with the extent of overestimation being dependant on the nature of the particle system.

In the approach presented here, our particle network is allowed to consolidate under gas pressure until $d\phi/dt = 0$ and $dH/dt = 0$, thus eliminating the complexities of dynamic cake behavior such as settling and consolidation. By taking this steady-state approach we show that it is possible to obtain the solid fraction profile by reducing Eq. 4 to

$$\frac{d\phi}{dz} = \frac{C}{D(\phi)} \tag{6}$$

where the solid fraction profile is only a function of the diffusivity $D(\phi)$. The diffusivity function $D(\phi)$ can be expressed in terms of the compressive yield stress $P_Y(\phi)$ and hindered settling function $R(\phi)$ as[8]

$$D(\phi) = \frac{(1-\phi)^2 \frac{dP_Y(\phi)}{d(\phi)}}{R(\phi)} \tag{7}$$

Given the steady-state filtration assumption, we develop a numerical technique to calculate the local solid fraction profile $\phi = f(z)$ based on compressive yield stress and permeability (analogous to the inverse of the hindered settling function). We then use this local solid fraction profile as the basis for evaluating our permeability and compressibility functions.

Gas driven filtration versus piston driven filtration

In submerged membrane filtration, suction pressure is applied at the outlet drawing the influent water through the membrane. This is similar to the classical laboratory gas driven filtration system, where gas pressure forces the fluid through the membrane and, in the process, compacts the material deposited on the cake.

Consolidation studies traditionally involve the use of a piston driven device where pressure is directly exerted on the particle network forcing the fluid out of the network and through the membrane. The manner in which the load is applied makes it an ideal choice for modeling the consolidation as the pressure exerted on the cake is uniform (i.e., does not vary spatially through the cake) allowing calculation of the local solid fraction directly. It is for this reason that a piston filtration approach has been chosen to validate our numerical "cake integration" approach.

A number of other investigators have used piston devices to measure compressibility and permeability characteristics of porous assemblages.[9,10] Although piston filtration is ideal for characterizing material properties, experiments are constrained by the piston geometry where it would be difficult to modify the filtration cell to accommodate in situ size measurement and/or shearing. This makes gas filtration desirable as there are less geometrical constraints and it is akin to the real world filtration process of interest. Hence, in this study, we utilize an approach to quantify the dewatering properties of a material based on gas filtration data.

Compressive yield stress $P_Y(\phi)$ and permeability $K(\phi)$

The permeability of a porous medium is a measure of how easily a fluid can pass through the medium. For single spheres arranged in a specified manner, this can be modeled by the Carman–Kozeny relationship;[11] i.e.

$$\frac{dP_L}{dz} = \frac{k\phi^2}{(1-\phi)^3 d_p^2 U_s} \tag{8}$$

where k is a constant, d_p is the particle diameter, P_L is the liquid pressure and U_s is the superficial fluid velocity. For flocculated material this is a poor estimation of the pressure drop as there is a wide distribution in cake pore size, leading to an overestimation of the pressure drop. In this work, we do not restrict ourselves to a particular model; rather, we choose an unrestricted functional form which suitably describes the permeability of a wide range of materials.

In the studies reported here we characterize the compressibility of filter cakes in terms of the compressive yield stress $P_Y(\phi)$, which is defined as the pressure required to compress a cake to a given solid volume fraction. This is valid anywhere above the point at which flocculated particles form a continuous network (gel point). For filtration, it is important to characterize the compressibility of our cake, as a small change in solid fraction can lead to a change in permeability of several orders of magnitude.[12]

There are numerous functional forms for compressive yield stress models. Amongst the most straightforward is the power law[13]

$$P_Y = \kappa\phi^{\gamma} \tag{9}$$

which has been observed to describe the compressibility of salt destabilized systems of zirconia. Physically, this model suggests that for every incremental increase in solid fraction, there is an increase in the number concentration of interparticle bonds for a given volume of cake. The force required to induce a yielding in the bond network appears to increase as a power law with solid fraction, where the magnitude of the exponent γ quantifies the strength of the particle network.

Smiles[14] also observed that for soils, the solid volume fraction varies with applied pressure in a logarithmic fashion though he parameterized this in terms of the moisture ratio (ϑ) and the overlying water head (ψ); i.e.

$$\vartheta = A - B\ \ln(\psi) \tag{10}$$

where

$$\vartheta = \frac{1-\phi}{\phi} \tag{11}$$

Similar behavior has been described for a variety of soil and clay type particles.[15] However, the suitability of this model for our systems is questionable since negative

moisture ratios are predicted at high solid pressures. Furthermore, the moisture ratio predicted as $P_S \rightarrow 0$ does not equate to the gel point moisture ratio due to the discontinuous behavior of the function at this limit. As a result of these inconsistencies, this model was considered unsuitable for our work.

Channel et al.[16] have shown that flocculated alumina nanoparticles exhibit nonpower law compressive yield stress. The results clearly show that cakes formed from highly flocculated material exhibit greater strength initially but then converge to a power law form at higher solid fractions. Similar behavior was observed by Gladman et al.[17] in studies of the dewatering of slurries treated with polymeric flocculants.

In studies reported here, an unrestricted functional form is used that encompasses all types of behavior. As described later in this paper, a model of logistic form is shown to be both suitable and convenient for the purpose of demonstrating the approach.

Review of other numerical approaches

A variety of alternate techniques to those used here have been developed to address the need for characterization of local filter cake properties that develop in pressure (or vacuum)-driven filtration systems.

Phillip[18] suggests a numerical method involving material coordinate transformation of Eq. 4. It is possible to predict the local cake properties using this technique if one assumes a moisture ratio versus pressure function of the form shown in Eq. 10.

Wakeman[19] suggests an integration technique for solution of the differential equations describing cake formation. This technique requires an intrusive method for determining liquid pressure through the cake (i.e. Pitot probe or similar) or alternatively using a resistivity technique. However, varying the initial solids concentration is likely to bias cake permeability for flocculated systems due to inconsistent floc size between measurements. Additionally, intrusive probes cannot be used for thin cakes.

Lu et al.[20] used a numerical technique for analysis of flux data. This approach gives local cake properties but is highly model-dependant and, as such, is not well suited to application across a wide range of materials and conditions. The Lu approach uses the Carman–Kozeny relationship to describe the expected pressure drop across a section of cake. This approximation is suitable for nonflocculated suspensions but, given the heterogeneity of pores in cakes formed from flocculated suspensions, it may well over estimate the pressure drop.

It is clear from this brief review that a more robust way of determining cake properties at a local level would be useful.

Theoretical Basis

A technique for quantifying the compressive yield stress and cake permeability from steady-state filtration data is described here. The key to this approach is the procurement of reliable and consistent filtration data and final cake heights or average moisture ratios. Using these values as input data, we perform a numerical integration over the cake depth to calculate the compressibility and permeability functions that most accurately reproduce the observed filtration behavior. The estimation of these dewatering properties is free of model assumptions and, as such, has the potential for quite general application.

Numerical integration overview

The numerical technique used here involves conceptualizing the total cake mass as an accumulation of discrete slices. A momentum balance is performed for each slice in a sequential manner. This is performed from the top of the cake to the bottom of the cake as the force external to a slice is exerted from above. On the basis of the assumption that the solid particles are not deformable, the momentum balance is given by

$$\frac{\partial P_L}{\partial z} = -\frac{\partial P_S}{\partial z} \tag{12}$$

where P_L is the local liquid pressure and P_S is the local solid pressure. The numerical cake integration procedure performs this force balance in a discrete manner on the basis of a slice of fixed mass. For each cake slice we define a pressure drop as follows

$$dP_L = \frac{J}{K(\phi)} dm \tag{13}$$

where dP_L is the trans-slice liquid pressure drop, J is the steady-state filtrate flux, which is a constant through all slices, dm is the incremental cake mass with units of kg/m^2 and $K(\phi)$ is the mass-based permeability, which we define for our study. The mass-based permeability compares to the Darcian permeability according to the following equation

$$K_d = \frac{K\mu}{\rho\phi} \tag{14}$$

where ρ is the particle density.

To quantify the local solid pressure P_S or liquid pressure drop ΔP_L relative to the applied pressure we integrate Eq. 13; i.e.

$$\Delta P_L = P_S = J \int_0^M \frac{dm}{K(\phi)} \tag{15}$$

where P_S is the cumulative solid pressure due to the force imparted by the cake (of mass M), dm is the nominal slice mass and J is the flux obtained from filtration experiments. Equation 15 is evaluated numerically as detailed in the Technical Appendix. By definition, the solid pressure corresponding to the equilibrium local solid fraction is equivalent to the compressive yield stress.

If we substitute our experimentally determined J values into Eq. 15 and select an appropriate form for function K then we expect the following criteria to be satisfied

$$P_{S,n} = \Delta P_J \tag{16}$$

where ΔP_j is the pressure applied during the steady-state filtration, which resulted in measured steady-state flux J_j where

subscript j denotes the particular filtration runs at 12.5, 25, 50, 100, and 200 kPa. To calculate the solid pressure exerted on the membrane, defined as $P_{S,n}$, we integrate according to Eq. 15 across the whole cake. Thus, we must first assume a form for $K(\phi)$ then iteratively refine its parameters such that the convergence criterion is met. In addition, a functional form of the solid fraction dependence on P_S (i.e., the inverse compressive yield stress function $\phi(P_S)$ is required for the numerical integration. The assumed forms for both $K(\phi)$ and $\phi(P_S)$ are detailed in the Technical Appendix.

For the correct $K(\phi)$ and $\phi(P_S)$, the criteria set by Eq. 16 must be met independent of applied pressure. To ensure that this is the case, filtrations are performed for at least five different nominal pressures ΔP_J and the best permeability and compressibility fits obtained to the complete data set.

A detailed explanation of the numerical technique used is given in the Technical Appendix.

For the reciprocal arrangement where the material properties are known, it is possible to calculate the filtrate flux by the procedure described here. An iterative procedure is required to calculate J such that the following relationship is obeyed

$$J\int_0^M \frac{dm}{K(\phi)} - \Delta P_J = 0 \tag{17}$$

where J is the calculated filtrate flux and ΔP_J is the applied filtration pressure.

Materials

The experimental component of this work involves the acquisition of filtration data for input to the "cake integration" procedure. For the experimental work three types of particles of distinctly different characteristics were chosen to validate the technique. For each particle system, pressure filtration studies were undertaken for at least five nominal pressures and a stepped pressure piston filtration study was performed to validate the deduced compressibility model. Additional comparisons between the model deduced from filterability studies and results obtained using a centrifuge technique were undertaken to validate the deduced model in the moderate to low pressure range. The permeability model was also validated using a compression-permeability (CP) device known as a Rowe Cell. The Rowe Cell differs from other odeometers in that there is provision for directly measuring the permeability of a sample in addition to determination of its compressibility.

Particle preparation

Two types of zirconia (ZrO_2) are used as model particles in this study, both of which have well behaved and reproducible characteristics. Zirconia has been used in numerous other compressibility studies.[9,10,13,16] The zirconia particles (Aldrich Chemical Company, Milwaukee, Wisconsin) possessed a specific density of 5.850 and exhibited mean particle sizes of 5 and 10 μm. The zirconia suspensions were prepared in 0.1 M KNO_3 with 10 mM sodium tetraborate tetrahydrate used to buffer the suspension at a stable nonflocculating pH of 8.8. Acetic acid (0.1 M) was added to the stirred zirconia suspensions to reduce the pH to the isoelectric point of pH 7.3 where flocculation occurred. For the zirconia system the steady-state floc sizes were approximately 90 μm for the 5 μm zirconia and 70 μm for the 10 μm zirconia as measured in situ by focused beam reflectance measurement (FBRM) using a Lasentec (model M400L-316K).

Yeast was also chosen for the validation work as an example of a soft biological particle typical of those found in wastewater treatment. Two types of yeast were chosen. Bakers yeast supplied by Tandaco was used, having a mean particle diameter of 5 μm and specific density of 1.40. Optimum flocculation for these yeast particles has been observed by the authors and other workers[21] to occur at pHs between 4 and 5. The floc size was approximately 120 μm as measured with the FBRM. Dried yeast supplied by Fluka was also used. While this material has similar mean particle size and specific density to the Tandaco yeast, particle size measurement indicated that smaller flocs occurred at pH 4.5 with mean floc size attained of <20 μm.

The preparation of yeast suspensions is somewhat more complex than that of zirconia. According to Hughes and Field,[22] it is necessary to wash the yeast as the transmembrane pressure rise for washed yeast cells has been found to be lower than that for unwashed yeast. For this reason, the yeast was dispersed in milli-Q water and sonicated with a high power sonicator (Model Misonix) for 5 min at intensity of 24 W in a volume of 0.5 L. Following sonication, the sample was centrifuged at 3,000 rpm and 10°C for 15 min using an Allegra 25R centrifuge. The supernatant was decanted and the yeast washed in a manner identical to the first washing procedure, except that sonication was undertaken with a Consonic Model SM 2200 sonicator as only a lower power sonication was necessary to redisperse the yeast. The washed yeast was resuspended in milli-Q water and flocculation induced by lowering the pH to approximately 4.5 with 0.1 M acetic acid dosed into a high shear environment created by a four blade axial impeller operating at 500 rpm. To encourage flocculation, the suspension was subsequently stirred with the impeller for 5 min at a reduced speed of 250 rpm.

A clay type soil material was also used in our studies. The soil is heterogeneous in nature (Tweed River, Queensland, Australia). This particle system was chosen to further illustrate the flexibility of the approach described above. The soil particle size was measured using forward light scattering and found to be polydisperse with a mean particle size of 15 μm. The soil was stored in its sampled state with care taken to maintain the moisture content close to that of the original sample. The soil exhibited a specific density of 2.6. The floc size varied between 50 and 60 μm as measured with the Lasentec FBRM.

The soil was prepared by dilution will milli-Q water to a solid fraction of 0.05 and a total volume of 200 mL. The soil was stirred at 1,000 rpm to disperse the particles. The stirring speed was lowered to 250 rpm and 0.1 M acetic acid added to bring the pH down to 3.5 in order to induce flocculation. Stirring was continued for 5 min.

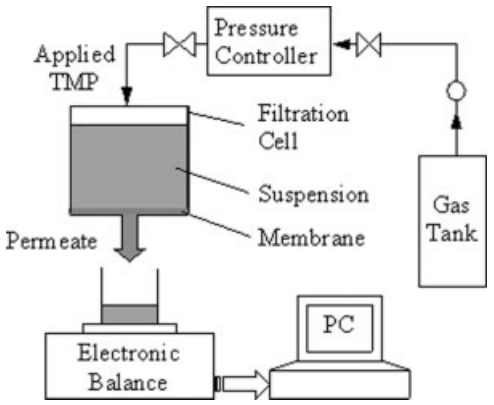

Figure 1. Experimental set-up used for filtration studies.

Methods

Filtration cell

Steady-state filtration data was obtained using the dead-end batch filtration cell shown in Figure 1. A pressure controller (Bronkhurst 602C) was used to maintain a precise and constant transmembrane pressure in the 12.5–200 kPa (± 0.1%) range, and filtrate flow data was logged using an electronic balance and standard PC. For all experiments, Sartorius 0.2 μm cellulose acetate membranes were used.

Experimental procedures. The flocculated suspension was poured into the filtration cell and allowed to settle. Depending on the system, the filter cake was allowed to consolidate for up to 30 min to within 5% of the expected steady-state height (Figure 2), where ϕ_g and ϕ_∞ represent the gel point solid fraction and solid fraction at $z = 0$ respectively. After consolidation, the system was pressurized, the valve opened and permeate mass sampled at fixed intervals. The filtration was continued until the flux reached steady-state at which point it was stopped.

Any remaining supernatant was removed with special care to ensure that the solid was not disturbed. The cake height was then measured using a volume displacement technique. This involved transferring the wet cake to a volumetric flask of suitable size with care taken to preserve the water within the cake structure. Water was then added to the volumetric mark and the volume of cake determined from the flask volume minus the volume of water added. With the volume of the cake known, the final cake height was calculated as follows

$$H_\infty = \frac{V_c}{A_c} \tag{18}$$

where V_c is the cake volume and H_∞ is the steady-state cake height. By using high particle loadings, cake volumes of around 20 cm^3 were typically formed. In general, the volume displacement technique relies on a sufficiently large cake to minimize measurement error. For thin cakes, a more precise technique would be necessary. It should be noted that it is important to stop the filtration before all the water is expelled from the filtration cell, as error is likely to be introduced if cake desaturation occurs. From direct observation of cake height in separate experiments, we have found that the error associated with this technique is within 3% at 20 mm and 5% with cakes of 10 mm thickness. This error arises from losses of material during separation of supernatant.

Compressive yield stress

Comparison measurements of the compressive yield stress were undertaken by piston filtration (odeometer) and centrifuge settling techniques.

Odeometer (rowe) cell. To validate the method described above, the Rowe Cell was used to directly determine the compressive yield stress for the materials of interest. For a piston driven system, the force applied by the piston is equal to the force of the interparticle bonds acting to oppose the compaction of the cake. As a result, the network stress is uniform throughout the cake leading to uniform cake porosity when the cake is at equilibrium. Given these conditions, we can calculate the solid fraction of the cake under piston load

$$\phi_f = \frac{\phi_o H_o}{H_f} \tag{19}$$

where ϕ_o is the initial solid fraction, H_o is the initial suspension height and H_f is the final cake height. Alternatively, ϕ_f can be measured by oven drying the wet cake. For piston filtration, the compressive yield stress is equal to the applied piston pressure corresponding to the equilibrium solid fraction ϕ_f.

Experimental equipment. The piston filtration device used in our studies is a Rowe Cell[23] of diameter 76.2 mm and recommended for sample heights of 30 mm. The cell itself consists of three parts: the body, the cover and the base. All three components are made of copper. The cell body is clamped between the base and cover by long tie-bolts as shown in Figure 3.

For the studies described here a 0.45 μm Millipore membrane on a thin polyester filter support was used. The piston pressure was regulated using a pressure controller (Bronkhorst 602C). The permeate exited the Rowe Cell at its base and was weighed on a computer-logged electronic balance.

Experimental procedures. The flocculated particles were poured into the Rowe Cell and the particles allowed to settle and consolidate under gravity. After consolidation the clear supernatant was removed using a syringe. To ensure constant pressure distribution over the filter cake, a thin aluminium metal plate was placed between the piston and the cake. Following closure of the cell top, pressure was applied at a start-

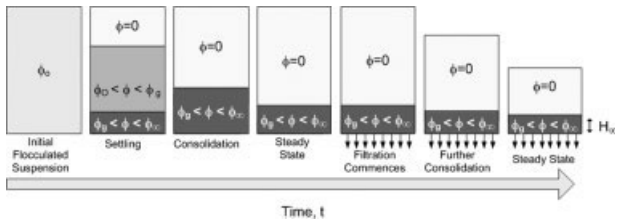

Figure 2. Time line showing consolidation to steady-state prior to filtration.

Filtration is commenced and run to steady-state (i.e. $dJ/dt = 0$).

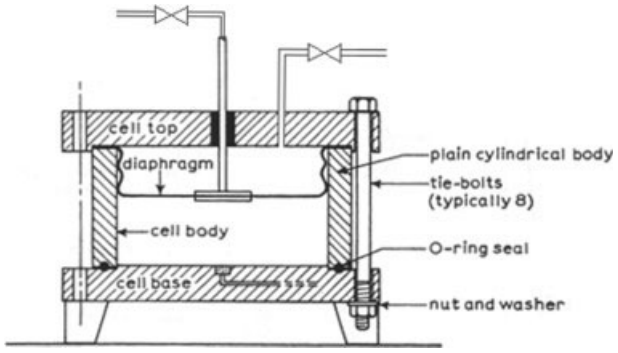

Figure 3. Rowe Cell cross section showing the assembled unit used to measure compressibility and permeability.

The pressure source connected to the centre channel of the piston is connected to fluid reservoir used for permeability measurement. The second pressure source (offset) is supplied to the diaphragm used for compressibility measurement.

ing value of 12.5 kPa and filtrate collected until no further liquid was expelled. The pressure was then stepped up to 25 kPa (then 50, 100, and 200 kPa) and the process repeated. The moisture ratio of the zirconia filter cake was obtained by oven drying at 120°C for 24 h. The moisture ratio of the yeast cake was best determined from cake volume as oven drying tends to remove cell water in addition to the free water. The cake height (and subsequently volume) was easily determined using a digital caliper. Knowing the final moisture ratio, the moisture ratios at the lower pressures could be back calculated by mass balance based on the volume of permeate expelled from the Rowe Cell at each pressure step.

The Rowe Cell filtration of zirconia was performed from a starting solid fraction of 0.06. The collected filtrate volume versus time data are shown in Figure 4 where the distinct stepped pressure phases during the filtration are evident. Initial consolidation times are typically 1–2 h depending on the material. Once the cake had consolidated to the equilibrium height at the initial pressure, subsequent pressure steps required about 15–30 min to reach equilibrium.

Equilibrium height settling tests (gravity and centrifuge)

The centrifuge used was a Spintron GT–175 with capacity for 16 tubes, top speed of 4,000 rpm, maximum volume of 4 × 250 mL and radius R of 160 mm. To ensure a constant radial stress distribution throughout the sample, it was necessary that flat bottomed tubes were used. Transparent, 50 mL conical bottomed centrifuge tubes were used with the flat bottom created by injecting a small quantity of silicone into each tube using a syringe. The silicone was allowed to set in an upright position for 24 h.

Experimental procedures. In the multiple speed equilibrium sediment height technique, the equilibrium sediment height H_{eq} and gravitational constant g are obtained. By using this raw data, $P_Y(\phi)$ and the solid fraction can be calculated using the mean value theorem of Buscall and White.[24] The mean value "approximate" solution for $P_Y(\phi(0))$ is a very good solution to the compression equation[25]; i.e.

$$P(0) \approx \Delta\rho\phi_o H_o g\left(1 - \frac{H_{eq}}{2r}\right) \tag{20}$$

$$\phi(0) \approx \frac{\phi_o H_o\left[1 - \frac{1}{2r}\left(H_{eq} + g\frac{dH_{eq}}{dg}\right)\right]}{\left[\left(H_{eq} + g\frac{dH_{eq}}{dg}\right)\left(1 - \frac{H_{eq}}{r}\right) + \frac{H_{eq}^2}{2r}\right]} \tag{21}$$

Particular experimental procedures were used for soil and yeast, as described below.

Soil: A defined volume of suspension was placed in a tube, typically to 90–95% of the tube capacity. The sample was then centrifuged for 30 min at a constant speed S. The supernatant was poured into a beaker and the tube with compacted soil weighed. To measure H_{eq}, water was added to the filter cake until there was a volume of 40 mL in the tube. The equilibrium sediment height could then be calculated by volume difference. The tube was weighed and the supernatant returned to the tube. The speed of centrifugation was then increased and the procedure repeated. Five to seven equilibrium heights for different speeds were required.

Yeast: The experimental procedure for yeast was almost identical to that used for soil except that the height was obtained by measuring the interface between the sediment and the supernatant and an average of the highest and lowest parts of the interface determined.

Permeability

Permeability of consolidated cakes was obtained using the Rowe Cell but operated in a different manner to that used for determination of compressibility. The principle behind the permeability measurement is to compress a known amount of material to steady-state with a known piston pressure. A second pressurized fluid source is connected to the Rowe Cell inducing fluid under pressure (the so-called "pore pressure") to pass through a channel on the centre axis of the piston towards the cake. By simultaneously applying a piston pressure and a pore pressure, it was possible to com-

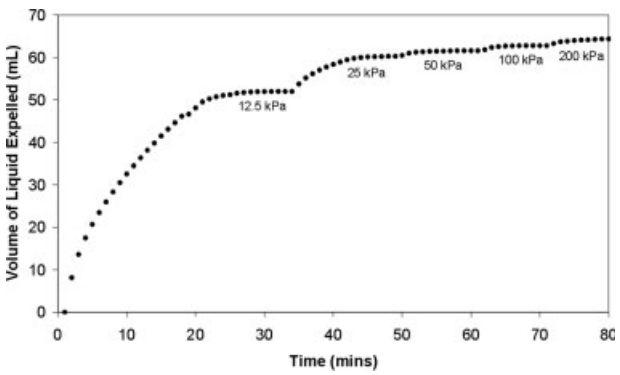

Figure 4. Rowe Cell filtrate collected as a function of time for the 5 μm Zirconia at pH 7.3.

Similar trends are observed for the other flocculated materials upon compression.

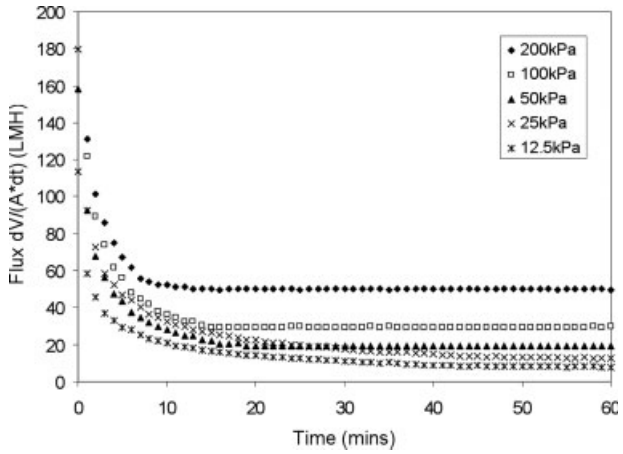

Figure 5. Filtration of zirconia illustrating the time it takes for steady-state flux to be reached.

Steady-state is typically reached within an hour.

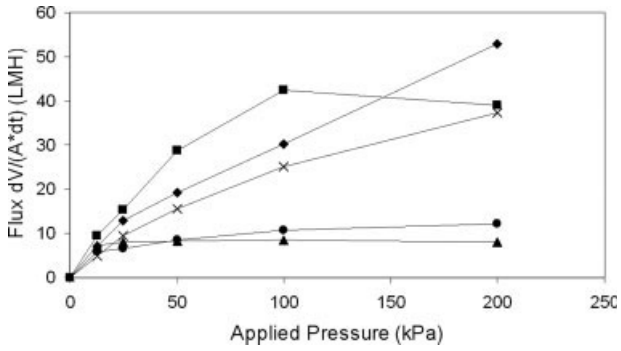

Figure 6. Steady-state flux vs. applied nominal pressures (■) flocculated yeast pH 4.5 (▲) smaller yeast flocs pH 4.5 (◆) 5 μm zirconia pH 7.3 (×) 10 μm zirconia pH 7.3 (●) soil pH 3.5.

press the material to a known solid fraction and to then force fluid through the cake. By simply rearranging Eq. 13, the permeability of the cake could be determined from the measured flux.

Prior to examining the permeability of the various particulate assemblages, a pure water flux test was run on the Rowe Cell with sintered plate, reservoir and filter paper in sequence. The calculated permeability was measured at several pressures and was consistent at 1.5×10^8 Pa/flux unit. This represents a pressure drop of less than 3% and was considered acceptable for the purposes of the investigation reported here.

Procedure. Particles were prepared as described previously and transferred to the Rowe Cell. The aluminium plate was replaced with a permeable sintered plate to allow passage of fluid. The sintered plate was underlain with a layer of filter paper to prevent particles from permeating back past the plate, and to provide a seal between the plate and the outer ring. The plate was then placed onto the consolidated material. Piston pressure was applied to the plate thereby consolidating the underlying material. Filtrate was expelled from the Rowe Cell until no further consolidation occurred (i.e. the steady-state flux was zero).

At steady-state, a solution of known composition held in a 2 L reservoir was passed through the cake by applying a defined pore pressure. In these studies, a solution of the same composition to that used in flocculation was employed to reduce the likelihood of cake rearrangement due to change in ionic strength or pH. The filtrate volume was logged at fixed intervals to enable calculation of the flux. According to Eq. 13, a constant flux is expected as the filtration is being performed at steady-state. $K(\phi)$ can thus be calculated based on the measured constant flux and applied pore pressure ΔP_L with ϕ obtained from the Rowe Cell compressibility experiment.

This procedure was repeated for each of the nominal pressures. For each pressure, equal pore and piston pressures were applied to minimize further consolidation.

Results and Discussion

Filtration

For each material, filtrations were performed separately over a range of nominal pressures. The filtrations were allowed to continue to steady-state (i.e. until there was no further change in flux). This is illustrated for zirconia in Figure 5, where it can be seen that filtration to steady-state typically takes approximately an hour. Filtration runs longer than 1 h was typically not necessary given the amount of material used.

A plot of the steady-state flux versus nominal applied gas pressure is given in Figure 6. For each system we see a trend expected for a compressible cake with a nonlinear relationship between flux and pressure. For both yeast systems we observe a maximum flux followed by a decrease at higher pressures. This maximum flux is referred to as the cut off flux above which compaction effects lead to reduced permeability and outweigh the effect of increased pressure. It is noteworthy that similar behavior is often encountered in water and wastewater treatment systems.

A summary of the calculated parameters are given in Table 1 with R^2 values indicating the quality of fit to the data.

Table 1. Summary of Parameters Calculated by Numerical Analysis of Steady State Filtration Data

	C_1	C_2	C_3	C_4	C_5	C_6	R^2
Zirconia 1	3.82E − 08	4.53	0.0137	0.0888	1.43	−1.69	1.000
Zirconia 2	3.31E − 08	3.62	0.0579	0.0557	3.45	−1.31	0.999
Yeast 1	3.45E − 09	1.84	−0.0238	0.00700	3.06	−0.710	0.988
Yeast 2[a]	1.26E − 06	7.09	0.0986	0.0797	0.55	−1.35	0.978
Soil	7.75E − 09	11.7	0.215	0.0349	10.4	−1.41	0.987

[a]Permeability functional form as $K = C_1 * (0.7 - \phi)^{C_2}$.

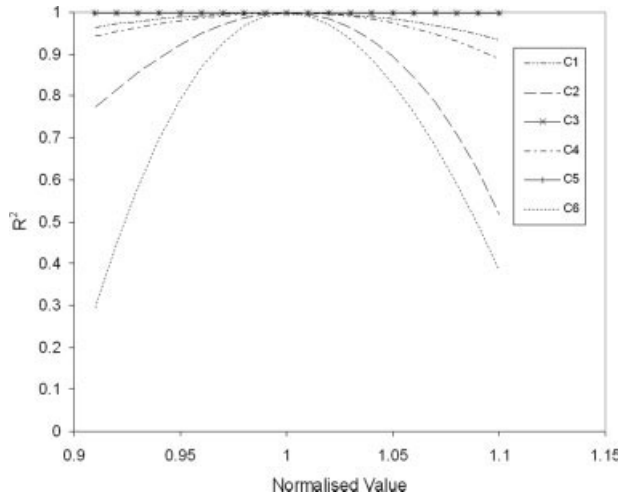

Figure 7. Sensitivity of correlation coefficient to change in optimum constant values for 5 μm zirconia.

These parameters are obtained directly from the output of the calculation for the analysis of each set of flux/pressure data for the five systems. For all systems there is an acceptable level of correlation with R^2 values close to 1 (see technical appendix for calculation). The sensitivity of the correlation coefficient to change in parameter value is shown in Figure 7 for the 5 μm zirconia system. These results show that particular parameters are less sensitive to variation in input data. If this is observed over a wide variation of input data for a certain system then it is possible to set the parameter as a constant. This can be useful as fewer data points are required to meet the required degrees of freedom for the analysis.

Compressive yield stress

The final solid fraction of the Rowe Cell compacted cake was measured by oven drying. As described earlier, the subsequent solid fractions for the lower pressures could be back calculated based on the volume of filtrate eluted at each pressure step. We were thus able to generate compressive yield stress versus solid volume fraction plots for each particle system of interest. The Rowe Cell compressibility data is compared with the values predicted from the numerical cake integration fits to the filtration data (indicated by the solid line) for the various particle systems of interest shown in Figure 8.

For the 5 μm zirconia (Figure 8), the predicted P_Y versus ϕ plot obtained from the converged model derived from the gas filtration data appears to agree well with the data obtained from the piston filtration studies in the moderate to high pressure range. There does not appear to be any systematic deviation of the model from the piston filtration data. The error bars indicate the uncertainty associated with the measurement of the solid fraction using direct cake height measurement. For the 10 μm zirconia (Figure 8), the converged model fit also appears to agree well with the piston filtration data. Similarly, results from the yeast filtration show a good fit against the Rowe Cell data in the moderate to high pressure range as shown in Figure 8. Error in the measurement of cake height propagates to the final result, but the model results typically fall within the expected range.

For the moderate to low pressure range, centrifuge experiments were performed to compare to our converged model fit. The results for the yeast exhibiting small floc size are shown in Figure 9 and demonstrate that the model derived from gas filtration data provides a good description of the compressibility of the material in this range.

All three techniques for measuring the compressive yield stress of the soil are overlaid in Figure 10 and demonstrate very similar P_Y versus ϕ behavior. This is particularly satisfying as each of the methods is quite independent of one another. A slight difference is apparent between the centrifuge and odeometer results, with the centrifuge technique indicating slightly higher solid volume fractions for a given applied pressure than is suggested by the odeometer analysis. The difference between these two methods of validation is most likely due to elastic deformation leading to an underestimate of the compressive yield stress to an extent that is difficult to quantify.

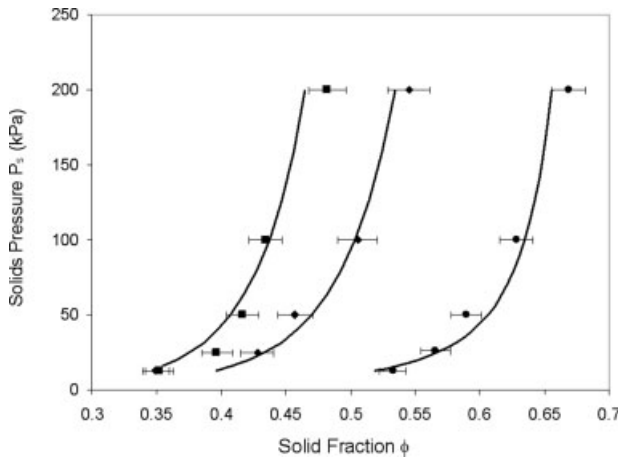

Figure 8. Comparison of the calculated compressive yield stress vs. direct measurement (■) 5 μm zirconia, (◆) 10 μm zirconia, (●) flocculated yeast.

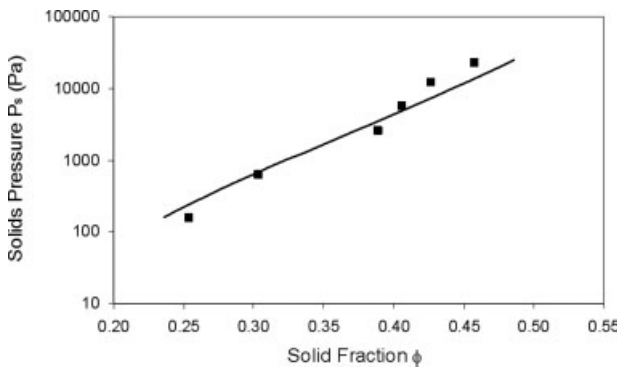

Figure 9. Comparison of the calculated compressive yield stress vs. centrifuge measurement for the smaller yeast flocs pH 4.5.

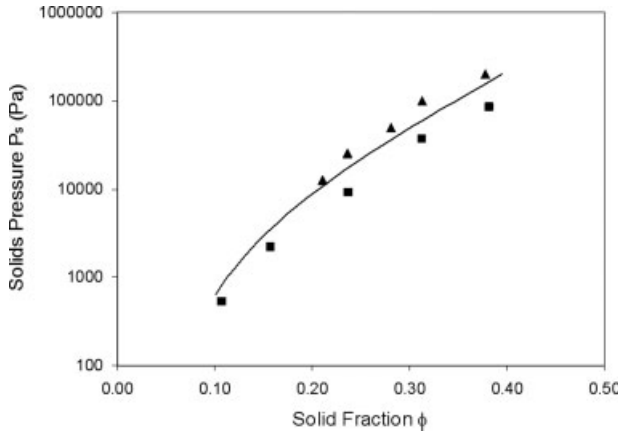

Figure 10. Comparison of the calculated soil compressive yield stress (solid line) vs. Rowe Cell (▲) and centrifuge measurements (■).

The choice of a logistic functional form for P_Y appears to be satisfactory for the range of particle systems examined in our filtration experiments with convergence of model parameters in all cases. Use of conventional power law forms such as Eq. 9 would not converge to an acceptable residual pressure in any of the systems. This illustrates that it is necessary to consider nonpower law behavior, particularly at low solid fractions when modeling filtration processes of flocculated systems. The functional form used here takes this low solid fraction behavior into account. At the same time it is shown to be convenient for the numerical analysis with only four parameters required to encompass the variety of behavior observed with minimal computational burden. It should be noted however that, although the logistic function used here is convenient, any functional form, including piecewise polynomial, could also be used.

Permeability

The permeability data obtained for zirconia, soil and yeast samples compressed to achieve a range of solid volume fractions as illustrated in Figure 11, along with the model predicted permeabilities for the various materials (derived from the gas-driven filtration runs). The predicted behavior is observed to be comparable to the Rowe Cell measurements for the flocculated yeast and zirconia. However, it is significantly higher than the Rowe Cell measurements for the soil system and lower than the Rowe cell measurement for the smaller floc size yeast. A possible explanation could be that both techniques calculate permeabilities that are accurate representations of the respective systems. It is also possible that there is a difference in the structure of the pores of the different cake materials, which arises from different flow histories which are unique to the nature of each technique. The most significant difference is the high initial flux that is common to gas filtration which, in our case, is approximately an order of magnitude higher than the steady-state flux for all materials. We do not observe this in our Rowe Cell filtration with steady-state flux being reached almost instantaneously as the consolidation process has been induced beforehand in a separate process (via the piston).

It is important to recognize that the technique described here is suitable for systems that exhibit a low cut off flux (as observed particularly for the small yeast flocs). Although the yeast exhibits quite normal compressive behavior, the permeability of the material, particularly at higher solid fractions, is several orders of magnitude lower than the other materials examined. This suggests that the pore size distribution of the small yeast flocs is much smaller than for the other material and is possibly more reflective of a nonflocculated system.

As shown by comparison with the Rowe Cell permeability measurements, the functional form selected to describe permeability is suitable for the range of solid fractions encountered in this study.

Cake height

The measured cake heights and corresponding calculated heights are compared in Figure 12. This figure shows good agreement between the experimental and calculated heights within the range of experimental error. For the larger cakes we observe less error by the volume displacement technique

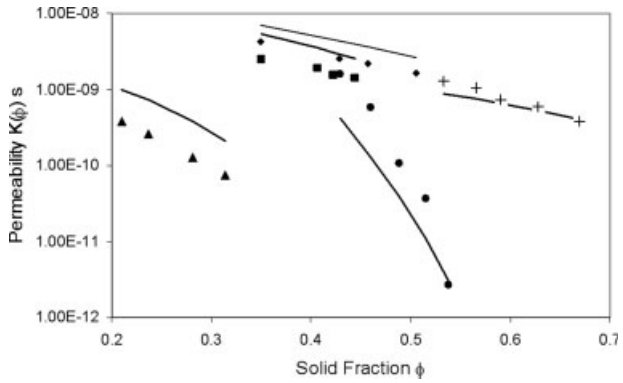

Figure 11. Permeability of cake material, measured directly versus the model fit for soil (▲), smaller yeast flocs (●), flocculated yeast (+), 5 μm zirconia (■) and 10 μm zirconia (◆).

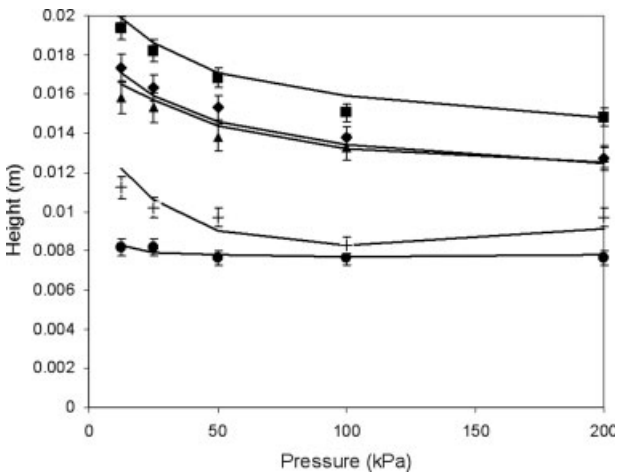

Figure 12. Comparison of measured cake height versus calculated ideal cake for soil (▲), smaller yeast flocs (●), flocculated yeast (+), 5 μm zirconia (■) and 10 μm zirconia (◆).

as we are working with larger volumes and losses in the transfer stage are proportionally smaller. Some points fall outside the range of error but it is stressed that the calculated fit here reflects the trend based on the best fit of the material parameters C_1 to C_6 to the gas filtration results.

Source of errors

Although the model fit calculated from the numerical cake integration provides comparable results to those determined by independent means, systematic and random errors are present. The most significant random error is due to the limitation in the accuracy of our cake height measurement. Random error in this measurement is typically less than 5%, depending on the final cake height. The error is magnified significantly for much smaller cakes and is thus the reason why solid loadings are selected that generates cake, which is greater than 5 mm in thickness. Other random errors arise as a result of differences in shear magnitude and pH between each filtration, however, caution was taken to minimize this.

Systematic errors arise from trapped air between the piston and the cake in the Rowe Cell technique. This certainly leads to higher than calculated solid fractions, as the dead volume of filtrate in the exit tube is expelled by air being pushed through the cake. In addition, the permeability dependence on flux history is postulated as the reason for the difference between the gas filtration-derived model and Rowe Cell results. To verify this we could manually limit the flux during the early stages of consolidation until steady-state appears to be reached before removing the imposed flow restriction.

Conclusion

A steady-state filtration technique has been described that appears to be suitable for characterizing cakes formed from flocculated materials. By driving gas filtration to steady-state we obtain stable flux data as input values for a numerical cake integration procedure. Model parameters for all particle systems examined had converged based on residual pressure minimization criteria and compared favorably to direct measurements of permeability and compressibility.

Estimation of the compressive yield stress based on the cake integration approach described here appears to be consistent with data obtained by odeometer (Rowe Cell) and centrifuge methods for all five particle systems examined. In addition, the calculated permeability for all systems is comparable to that predicted by the gas filtration-derived model. This suggests that the model forms used here for both the permeability (power law) and compressibility (logistic function) are suitable for this type of application. It is stressed that the model selection is not restricted to these functions and can essentially be of any form provided that the ideal calculated flux gives a reasonable fit to the experimental data.

Acknowledgment

The Australian Research Council and industrial partners Veolia Water Australia and Anjou Recherche (France) are thanked for financial support of this project.

Notation

A_c = cake area (m^2)
A = smiles constant
B = smiles constant
c_s = solid volume concentration (Kgm^{-3})
C = arbitrary constant
C_1,C_2 = permeability function parameters
C_3,C_4,C_5,C_6 = compressibility function parameters
d_p = particle diameter (m)
D = diffusivity (m^2s^{-1})
g = gravitational constant (ms^{-2})
H = cake height (m)
H_f = final cake height-piston filtration (m)
H_∞ = equilibrium cake height-gas filtration (m)
H_o = initial cake/sediment height (m)
i = subscript denoting cake slice number
J = flux ($Lm^{-2}hr^{-1}$)
K = permeability (s)
m = cake mass per unit area (Kgm^{-2})
M = compressibility exponent
M_i = cumulative cake mass per unit area (Kgm^{-2})
n = subscript denoting slice adjacent to membrane
N = compressibility exponent
P_Y = compressive yield stress (Pa)
P_S = solids pressure (pa)
P_L = liquid pressure (pa)
ΔP = liquid pressure drop (pa)
r = radius (m)
R = hindered settling function (Pasm−2)
R_c = cake resistance (m^{-2})
R_M = membrane resistance (m^{-1})
U = superficial fluid velocity (ms^{-1})
V = cumulative filtrate volume (m^3)
z = cake position perpendicular to filter plane (m)
α = specific cake resistance (mKg^{-1})
β = fitting parameter
ε = residual pressure (Pa)
ϕ = solid volume fraction
ϕ_o = initial solid volume fraction
ϕ_f = final solid volume fraction
ϕ_g = gel point final solid volume fraction
μ = dynamic viscosity (Pas)
ρ = solid density (kgm^{-3})
ψ = applied pressure (m H_2O)
ϑ = moisture ratio

Literature Cited

1. Landman KA, White LR. Solid/liquid separation of flocculated suspensions. *Adv Colloid Interface Sci* 1994;51:175–246.
2. Miller KT, Melant RM, Zukoski CF. Comparison of the compressive yield response of aggregated suspensions: Pressure filtration, centrifugation, and osmotic consolidation. *J Am Ceramic Soc* 1996;79:2545–2556.
3. Potanin AA, Russel WB. Fractal model of consolidation of weakly aggregated colloidal dispersions. *Phys Rev E* 1996;53:3702–3709.
4. Darcy H. *Les Fontaines Publiques de la Ville de Dijon*. In: Paris: Victor Dalmont; 1856:647.
5. Tiller FM. The role of porosity in filtration—Numerical methods for constant rate and constant pressure filtration based on Kozeny law. *Chem Eng Prog* 1953;49:467–479.
6. Landman KA, White LR. Predicting filtration time and maximizing throughput in a pressure filter. *Aiche J* 1997;43:3147–3160.
7. Landman KA, White LR, Eberl M. Pressure filtration of flocculated suspensions. *Aiche J* 1995;41:1687–1700.
8. Landman KA, Stankovich JM, White LR. Measurement of the filtration diffusivity D(phi) of a flocculated suspension. *Aiche J* 1999;45:1875–1882.
9. de Kretser RG, Usher SP, Scales PJ, Boger DV, Landman KA. Rapid filtration measurement of dewatering design and optimization parameters. *Aiche J* 2001;47:1758–1769.
10. Usher SP, De Kretser RG, Scales PJ. Validation of a new filtration technique for dewaterability characterization. *Aiche J* 2001;47:1561–1570.
11. Carman PC. Permeability of saturated sands, soils and clays. *J Agri Sci* 1939;29:262–273.

12. Waite TD, Schafer AI, Fane AG, Heuer A. Colloidal fouling of ultrafiltration membranes: Impact of aggregate structure and size. *J Colloid Interface Sci* 1999;212:264–274.
13. Green MD, Boger DV. Yielding of suspensions in compression. *Ind Eng Chem Res* 1997;36:4984–4992.
14. Smiles DE. A theory of constant pressure filtration. *Chem Eng Sci* 1970;25:985–996.
15. White I, Smiles DE, Santomartino S, van Oploo P, Macdonald BCT, Waite TD. Dewatering and the hydraulic properties of soft, sulfidic, coastal clay soils. *Water Resour Res* 2003;39(10).
16. Channell GM, Miller KT, Zukoski CF. Effects of microstructure on the compressive yield stress. *Aiche J* 2000;46:72–78.
17. Gladman B, de Kretser RG, Rudman M, Scales PJ. Effect of shear on particulate suspension dewatering. *Chem Eng Res Des* 2005;83(A7):933–936.
18. Philip JR. Numerical solution of equations of the diffusion type with diffusivity concentration-dependent. *Trans Faraday Soc* 1955;51:885–892.
19. Wakeman RJ. Numerical-integration of differential-equations describing formation of and flow in compressible filter cakes. *Trans Inst Chem Eng* 1978;56:258–265.
20. Lu WM, Huang YP, Hwang KJ. Methods to determine the relationship between cake properties and solid compressive pressure. *Sep Purif Technol* 1998;13:9–23.
21. Jin YL, Speers RA. Flocculation of *Saccharomyces cerevisiae*. *Food Res Int* 1998;31:421–440.
22. Hughes D, Field RW. Crossflow filtration of washed and unwashed yeast suspensions at constant shear under nominally sub-critical conditions. *J Membr Sci* 2006;280:89–98.
23. Head KH. *Manual of Soil Laboratory Testing*. London: Pentech Press, 1980.
24. Buscall R, White LR. The consolidation of concentrated suspensions. I. The theory of sedimentation. *J Chem Soc Faraday Trans I* 1987;83:873–891.
25. Green MD. *Characterization of suspensions in settling and compression* [PhD]. Department of Chemical Engineering, University of Melbourne, Melbourne, 1997.

Technical Appendix: Numerical Integration Procedure

The numerical integration of Eq. 15 is performed in discrete slices denoted by subscript i from $i = 0$ (top of cake) to $i = n$ (slice adjacent to membrane). Before we evaluate our model parameter guess we must generate the synthetic properties for each slice, namely the solid fraction ϕ_i. To achieve this we simulate the process of consolidation under pressure to achieve a cake, which is at steady-state. We also introduce the compressive yield stress function $P_Y(\phi)$ in combination with the numerical integration to calculate the solid fraction for successive slices. The process of consolidation is done via the following iterated procedure

1. Assume initially that the entire cake is at the gel point solid fraction ϕ_g by assigning this solid fraction to each slice.

2. The calculations described in steps 2 to 4 are performed for each slice starting at $i = 0$ (top). First we impose the experimentally measured steady-state flux J_j and calculate the pressure drop corresponding to the current slice $dP_{L,i}$ (Eq. 13). For this calculation we define a permeability function of the power law form

$$K(\phi) = C_1(1-\phi)^{C_2} \tag{A1}$$

where C_1 and C_2 are model parameters. It is stressed that the choice of functional form is flexible and this assumed form is one of many possible forms.

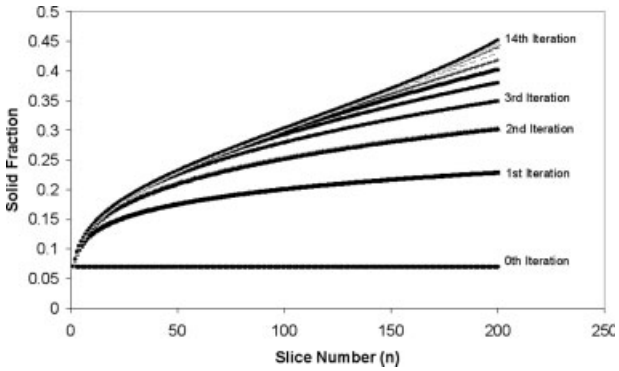

Figure A1. Typical Iteration for consolidating zirconia.

3. We then perform the integration of Eq. 15 numerically to calculate the pressure on the next slice $i + 1$.

$$P_{S,i+1} = \int_0^{M_i} \frac{J}{K(\phi)} dm = \Delta P_i + \Delta P_{i-1} + \cdots + \Delta P_o \tag{A2}$$

where M_i is the sum of cake mass above and including the current slice.

4. On the basis of the compressive yield stress function and the imposed solid pressure calculated by Eq. A2 we then calculate the solid fraction of the next slice $i + 1$. For our work we choose a compressive yield stress function of the logistic form

$$\phi_{i+1} = \left[\phi_{cp} - \frac{1 + C_3 e^{\frac{-P_{S,i+1}}{C_5}}}{1 + C_4 e^{\frac{-P_{S,i+1}}{C_6}}}(\phi_{cp} - \phi_g)\right] \tag{A3}$$

where ϕ_{cp} is the theoretical closed packing solid fraction or solid fraction at $P_S = \infty$, and C_3, C_4, C_5, and C_6 are model parameters. Here, the substituted value for P_s is $\log_{10}(P_s)$. The value for ϕ_{cp} is taken to be 0.7.

It is again stressed that the choice of functional form is flexible. This assumed form is suitable for the range of materials characterized in our work.

If we repeat the process of steps 2–4 sequentially for each slice from $i = 0$ to $i = n$ we can calculate the solid fraction profile of the entire cake.

5. We calculate the residual pressure $\Delta P_{Res,j}$ as follows

$$\Delta P_{Res,j} = \Delta P_j - P_{S,n} \tag{A4}$$

where $P_{S,n}$ is the solid pressure imposed by the entire cake at the final slice $i = n$ and ΔP_j is the experimental trans-cake pressure drop. On the basis of the calculated solid fraction profile we re-calculate each solid fraction again by repeating steps 2–4 until the change in residual pressure $\Delta P_{Res,j}$ does not differ by >0.1% with successive iterations. At this point the cake is at steady-state. Figure A1 illustrates a typical iteration.

To test the consistency of the model guess we substitute the same $K(\phi)$ and $P_Y(\phi)$ functions for several pressures. The loop is run for each of the nominal pressures used in our gas filtration experiment 12.5, 25, 50, 100, and 200 kPa and

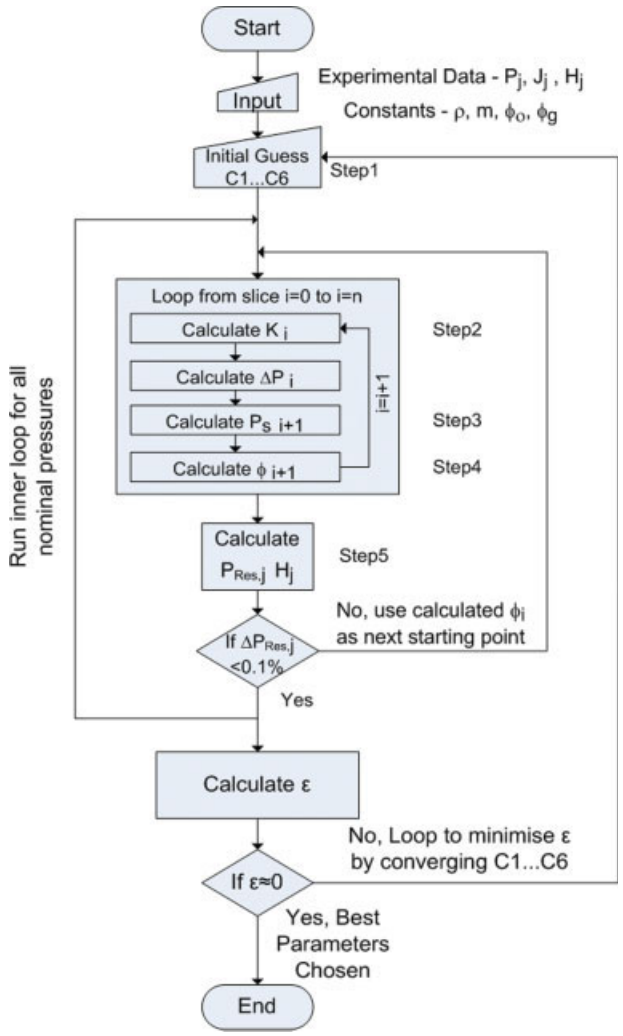

Figure A2. Flow diagram of procedure for selecting the optimum model parameters.

[Color figure can be viewed in the online issue, which is available at www.interscience.wiley.com.]

flux obtained. If the residual pressure is approximately equal to actual filtration pressure for each run such that $\Delta P_{\mathrm{Res},j} = 0$ for all j, then we can conclude that our model parameters are correct.

To assess the accuracy of the chosen parameters for our permeability and compressibility model we do a sum of square error such that

$$\varepsilon = P^2_{\mathrm{Res,\ 12.5}} + P^2_{\mathrm{Res,\ 25}} + \cdots + P^2_{\mathrm{Res,\ 200}} \tag{A5}$$

The key to the numerical integration technique is to converge the parameters $C_1 \ldots C_6$ such that we minimize the sum of square error ε.

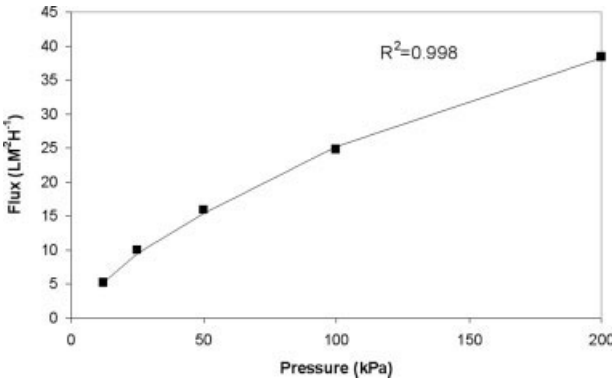

Figure A3. Goodness of fit of experimental data (■) to ideal flux trend (solid line) calculated based on zero residual pressure for 10 μm zirconia.

The parameter convergence process is managed using a nonlinear unconstrained optimization tool in MATLAB called fminsearch. By setting up the cake integration as a parameter optimization problem we can quickly converge to the most likely fit.

Additional weight is given also to converge the parameters according to matching the measured cake height with the calculated cake height H_∞, given by

$$H_\infty = \sum_{i=0}^{n} \frac{dm}{\rho \phi_i} \tag{A6}$$

where ρ is the solid density and dm is the mass of cake in slice i. This is crucial to obtaining a unique solution, as it reduces the degree of freedom in the calculation. Thus, particular care must be taken with the cake height measurement post-filtration, especially with materials which form cakes which have a tendency to break off.

A schematic of the algorithm is given in Figure A2. Typically convergence takes around 5 min depending on the accuracy of the starting point guess.

A measure for the goodness of fit for the 6 parameters is given using the correlation coefficient R^2. A separate iteration as given by Eq. 17 is performed to back calculate the "ideal" flux values given the 6 parameter fit, which is then assigned as our predicted response values. These ideal values are calculated based on zero residual pressure and hence is a theoretical perfect fit. On the basis of this we calculate a sum of squares due to error and routinely calculate an R-square correlation coefficient as a measure of the goodness of fit for our converged parameters. This is illustrated in Figure A3.

Manuscript received Sept. 27, 2006, revision received Jan. 16, 2007, and final revision received Apr. 3, 2007.